

Hot Superdense Plasmas and Fast-Electron Jets from Intense Femtosecond Laser Pulses

K. Witte 1), U. Andiel 1), K. Eidmann 1), E. Fill 1), C. Gahn 1), I. Golovski 2), D. Habs 3), R. Mancini 2), J. Meyer-ter-Vehn 1), G. Pretzler 1), A. Pukhov 1), R. Rix 1), T. Schlegel 1), and G. Tsakiris 1)

1) Max-Planck-Institut für Quantenoptik, Hans-Kopfermann-Straße 1, D-85748 Garching

2) Department of Physics, University of Nevada, Reno NV 89557-0058, USA

3) Sektion Physik, LMU München, Am Coulombwall 1, D-85748 Garching

e-mail contact of main author: klaus.witte@mpq.mpg.de

Abstract. With high-contrast light pulses of ≤ 200 -fs duration focused to intensities of $\geq 10^{18}$ W/cm², strongly coupled plasmas at solid state density and temperatures of a few 100eV can be generated. These plasmas are similar to those currently achievable only in indirectly imploded gas-filled microspheres during stagnation. The table-top size and high-repetition rate of the lasers producing these ultra-short pulses provided in our case by the 2-TW facility ATLAS allow to systematically investigate the basic features of these plasmas. First the mechanism of the dense-plasma generation is discussed. This is based on hydrocode and PIC simulations as well as on measurements of light absorption and the energy transport into the target. We then present spectrally and time-resolved measurements of the K-shell emission from aluminum targets. By fitting synthetic spectra obtained from code simulations to the experimental ones, it can be inferred that the plasma has an electron density of $\sim 10^{24}$ /cm³ and a temperature of ~ 300 eV.

In the fast-ignitor concept, a laser-generated electron jet is expected to ignite the central spot of the compressed target. Using ATLAS pulses focused to on-target intensities of 10^{18} - 10^{19} W/cm², we investigate the e-beam generation mechanism in preformed under-dense plasmas. A new fast-electron acceleration mechanism is identified.

1. Introduction

Ultra-short laser pulses have recently demonstrated that they can isochorically heat matter to temperatures of a few hundred eV thereby generating strongly coupled plasmas whose electron density exceeds 10^{23} /cm³ [1, and ref. cited therein]. Such plasma conditions are otherwise only achievable in indirectly imploded microspheres during stagnation [2] requiring multi-10 kJ laser facilities which can fire a few shots per day only. Lasers delivering femtosecond pulses have, however, a much higher repetition rate. It is this feature which makes them attractive tools for a *systematic* investigation of these hot dense plasmas.

In section 2, we first explain the physics of isochoric heating and then report an experiment in which we irradiate a solid aluminum target covered with a thin carbon layer with high-contrast (achieved by frequency doubling) 150-fs pulses from our ATLAS (Advanced Titanium:Sapphire Laser) facility which are focused to intensities, I , beyond 10^{18} W/cm². A thin surface layer of the aluminum is thereby converted into a hot dense strongly coupled plasma whose characteristic feature is the K-shell emission in the wavelength range from 6 to 8 Å originating from aluminum ions still keeping one, two, or three electrons. By fitting time-integrated synthetic spectra obtained from an upgraded version of the early Mancini code [3] to those measured, we infer an electron temperature, T_e , of ~ 300 eV and an electron density, n_e , of $\sim 10^{24}$ /cm³. The latter value is the highest obtained so far with fs-laser pulses. We also report time-resolved measurements of various lines within the K-shell emission band.

The second topic addressed in this paper is related to the fast-ignitor concept [4]. Here, the key issue is the electron jet which is generated by an ultrashort high-intensity pulse interacting with the coronal plasma. The e-beam is expected to tunnel through the high-density plasma

encapsulating the DT fuel and to deposit its energy in the hot spot thereby providing ignition. Our investigations are related to the e-beam characteristics and its generation mechanism. In section 3, we first present the results of our experiment in which a 790-nm/200-mJ/130-fs ATLAS pulse focused to intensities of $\sim 5 \times 10^{18} \text{ W/cm}^2$ irradiates an underdense hydrogen or helium plasma at almost critical density. The electrons emerging out of the plasma with an average energy of $\sim 5 \text{ MeV}$ are rather well collimated. We identify a new electron acceleration mechanism which we term direct laser acceleration (DLA). It is different in nature from the well known laser wake-field acceleration (LWFA) mechanism.

2. Isochoric Heating of Matter

When an intense short laser pulse irradiates a metal target, a thin surface layer is first heated whose thickness corresponds to the skin depth which is about 7nm for cold aluminum. This layer then expands with the ion sound velocity. A typical value reached at an intensity level of 10^{16} W/cm^2 is 10nm/100fs. On the time scale of the ATLAS pulse, expansion of the skin layer is hence no longer negligible. This fact does, however, not exclude isochoric heating of the solid matter. Besides the expansion, there also exists an electronic heat wave which transports energy into the target. Fig.1 describes the scenario obtained from simulations performed with the hydrodynamic code MULTI-fs [5]. As in the experiment, a p-polarized light pulse of 150-fs duration and 400-nm wavelength irradiates the target at an incidence angle of 45° and a focused intensity of 10^{17} W/cm^2 . Because the plasma density is thinned upon expansion, a layer with the critical electron density can develop where the laser energy is absorbed. Thereby a thin hot plasma located in front of the unexpanded solid is formed with a temperature of several keV. The fast electrons produced in the absorption layer penetrate into the solid. They set up a diffusive heat wave because their mean free path of a few nm is much shorter than the heat wave penetration depth which exceeds 100nm. Hence the electrons thermalize in the region traversed by the heat wave. Fig.1 is a snapshot 100fs after the pulse maximum. Later when the pulse is terminated, the hot low-density plasma cools down rapidly. On the other hand, the heat wave continues to further propagate through the solid resulting in a life time of the dense plasma of a few picoseconds before it also expands and cools down.

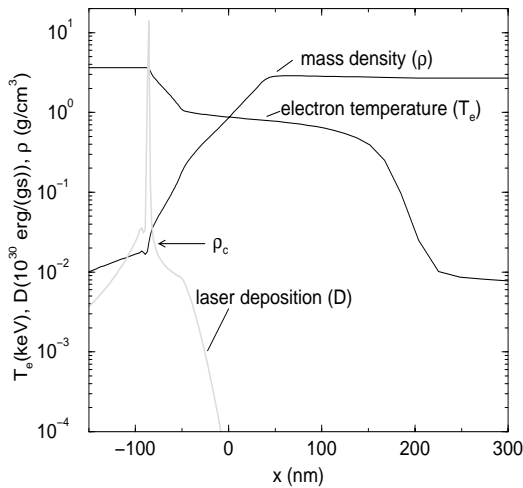


FIG.1. Spatial dependence of the mass density, electron temperature, and laser energy deposition 100 fs after the pulse maximum. The pulse (10^{17} W/cm^2 with 150-fs FWHM) comes from left. Initially, the target surface is at $x=0$.

At normal incidence, the absorption decreases with increasing intensity because in a hot plasma the electron-ion collision frequency is inversely proportional to three-half of the electron temperature. At intensities beyond 10^{17} W/cm^2 , the absorption is hence small and below 10%. However, more efficient absorption can be achieved by using oblique incidence and p-polarized light pulses. This has been experimentally demonstrated by several groups and is also reproduced by MULTI-fs and PIC simulations [5]. The absorption increases with the angle of incidence reaching a maximal value of $\sim 65\%$ at an angle of $\sim 70^\circ$. In contrast, the absorption for s-polarized light remains low at $\sim 10\%$ for all angles. The reason for the large difference between s- and p-polarized light is resonance absorption, a well known mechanism

in laser-generated plasmas. It is caused by the electric field of the pulse which is along the plasma density gradient at the critical layer. Plasma oscillations or plasma waves can then be excited. Collisions are negligible under this condition.

The penetration depth of the heat wave in the dense Al target as predicted by MULTI-fs (see also Fig.1) was measured by overcoating a NaCl substrate with Al layers of different thicknesses and observing the emission of Na K-shell lines as function of the Al layer thickness. The penetration depth corresponds to that Al layer thickness at which the Na K-shell emission begins to disappear. Typical values range from 100 to a few hundred nm and are well reproduced by MULTI-fs.

The electron density and temperature in the dense Al plasma is of particular interest. Information as to these entities is contained in the Al K-shell emission in the wavelength range from 6.0 to 8.4 Å (from the Ly-β to the K-α lines). The corresponding spectrum was measured (see Fig.2) using a von Håmos spectrometer supplied with a pentaerythritol (PET) crystal and recorded on a photographic x-ray film with an overall resolution of $\lambda/\Delta\lambda$ better than 1500. In order to keep the expansion of the Al plasma small, the Al surface is covered with a thin carbon layer of 45 nm thickness. Since carbon has no lines in the wavelength interval from 6.0 to 8.4Å, the Al spectrum is not spoiled by the presence of carbon. In order to efficiently absorb the laser radiation, the target is irradiated at an incidence angle of 45°.

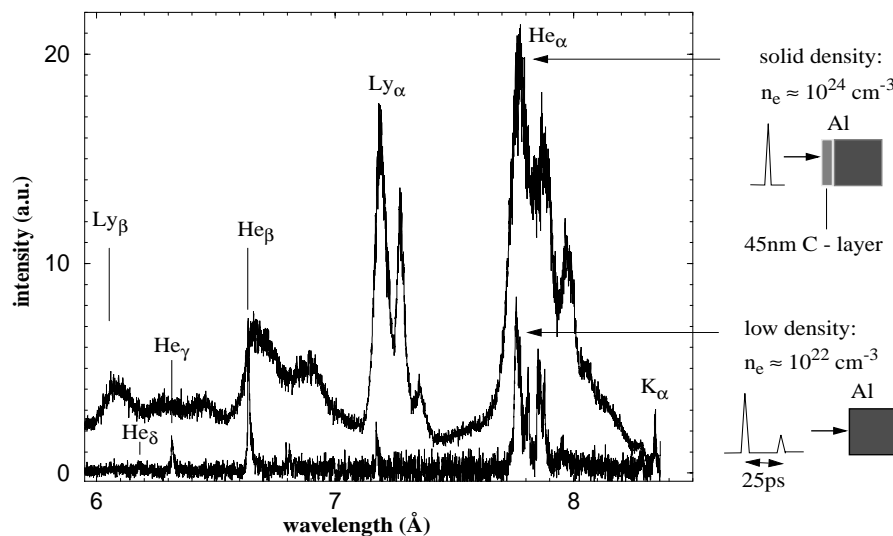


FIG.2.
Al K-shell
spectra mea-
sured at low
and high
density.

Fig.2 compares two spectra, one recorded at high and the other at low density. The low-density spectrum was generated by adding a prepulse preceding the main pulse by 25ps and using a massive Al target. The plasma created by the prepulse is therefore rather thin when the main pulse runs into it. The spectrum resulting from this interaction is hence characterized by sharp resonance lines designated as Ly-β, He-δ, He-γ, He-β, Ly-α, and He-α. On the contrary, the high-density spectrum produced from the carbon-overcoated Al target using a single pulse only becomes very broad due to Stark broadening. In addition, strong satellite contributions show up arising from transitions with an additional so-called bound spectator electron in levels with $n \geq 2$. This partially shields the nucleus potential. Transitions in presence of such a spectator electron are hence red-shifted as to the resonance lines.

The K-α line is emitted from a region deeply located inside the Al target where the matter is cold and not ionized. Release of a K-shell electron can here happen by impact of a fast elec-

tron or by x-ray photons. Subsequently, a transition of an L-shell electron into the hole in the K-shell gives rise to the K- α emission. The faintness of the K- α line indicates a low level of fast electrons. Since the K- α line is neither broadened nor shifted, it is used for wavelength calibration and the exact determination of the position of the various other lines in the spectrum shown in Fig.2. Thereby a red shift of the lines of the high-density case as to those of the low-density case becomes apparent. F. e., Ly- α is red-shifted by $\sim 15\text{m \AA}$ or 3.5eV . A line shift of 3.2eV is predicted by quantum-mechanical impact theory [6] for $T_e = 300\text{eV}$.

The theoretical calculation of the spectrum shown in Fig.2 or parts of it is rather complicated and only numerically accessible since a huge number of levels and transitions have to be accounted for. As an example of the analysis, Fig.3 compares the measured Ly- α line and the pertaining He-like and Li-like satellites with the corresponding synthesized lines. The simulations assume steady-state conditions and contain n_e and T_e as free parameters. Only optically thin lines such as the He- and Li-like satellites are suited for comparison. Best agreement is obtained for $n_e = 7 \times 10^{23}/\text{cm}^3$ and $T_e = 380\text{eV}$ at a red-shift of 4.3eV in accordance with [6]. This shift is somewhat larger than that from Fig.2 due to a higher intensity. The values found for n_e and T_e confirm previous results [1]. The confidence that from the analysis of the satellite-line shapes n_e and T_e can indeed be correctly inferred is further supported by the finding that when fitting the measured line shifts for Ly- α , He- α , and He- β with the theoretical ones [6] using again n_e and T_e as free parameters we arrive at the same values as before.

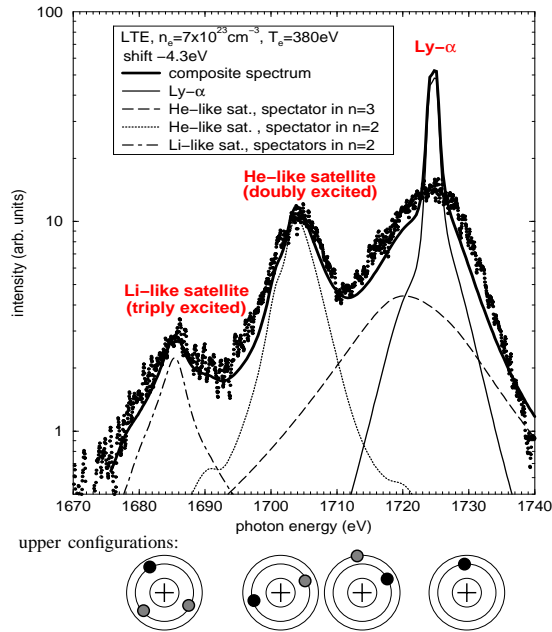


FIG.3. The Ly- α line with its satellites (measured data are from Fig.2). The lower part indicates the contributions considered in the calculations: Ly- α (right), He-like satellites with one spec-tator electron in either $n=2$ or 3 , and the Li-like satellites with two spectator electrons in $n=2$.

K-shell emission, a large number of shots had to be accumulated in order to improve the signal-to-noise ratio. For that, the camera had to be operated in a jitter-free triggering mode by applying semiconductor switches triggered by the laser pulse. The time resolution in this mode is 1.7ps . Correcting the measured pulse durations with this value, we obtained the

However, the Ly- α line is poorly reproduced. This discrepancy could not be resolved yet. Experiments with sandwich targets rule out arguments related to optical thickness. Reasons why the simulations miss the experimentally observed broad width could be higher-order satellites, temporal changes, and density gradients which are all not considered in the present theoretical model. The clarification of these open questions remains for future work.

The He- β and Ly- β lines are of relevance for ICF pellets in which a small amount of Ar serving as a tracer is added to the hydrogen filling. During stagnation, the conditions in the hydrogen plasma are similar to those in our Al plasma so that Ar K-shell emission can be observed. The He- β and Ly- β lines are selected to determine n_e and T_e [2]. Our investigations are hence a useful supplement to this topic.

The duration of the K-shell lines has been measured using an ultra-fast x-ray streak camera. Its time resolution is $< 1\text{ps}$ for single-shot recording. Due to the low intensity of the

following results: K- α and He-like satellites of Ly- α 1.2ps, Ly- α 1.3 ps, Li-like satellites of Ly- α 1.7ps, and He- α 2.1ps. The pulse shapes and durations obtained from MULTI-fs and the atomic kinetics code FLY agree fairly well with the streak camera data. The streaks of the double-pulse irradiation case also clearly prove the red shift of the Ly- α and He- α lines.

3. Fast Electron Jets

Hydrogen or helium gas-jet targets are well suited to generate fast-electron jets. The pulse leading edge creates the plasma in which the rest of the pulse undergoes relativistic self-focusing causing the formation of a light-guiding super-channel of a few λ in diameter and extending over tens of Rayleigh lengths [7]. The fast electrons originate in this channel. Their energy distribution is Boltzmann-like with an effective temperature, T_{eff} , which scales with $I^{1/2}$. In a helium plasma irradiated with 10^{18}W/cm^2 , T_{eff} reaches 5MeV. The faster the electrons, the better they are collimated: 1-MeV electrons are emitted in a cone with an apex angle of 16.5° , for those with 11MeV the angle reduces to 9.5° . For $T_{\text{eff}} \cong 5$ MeV, the total number of MeV-electrons is 2×10^{10} , corresponding to a total current of 15kA and a conversion of 5% as to laser energy. The PIC code simulations [7] show that most electrons experience DLA. However, this finding does not explain how DLA works in detail. Considering the trajectory of a single electron [8] improves the understanding. The PIC code simulations reveal that besides the laser field the electrons inside the channel are also subject to two strong quasistatic fields: An azimuthal magnetic field and an electric field pointing in the radial direction. In presence of these two fields only, the electron would move along the channel oscillating transversely with the frequency $\omega_{\perp} \approx \omega_p / (2\gamma)^{1/2}$, where ω_p is the channel plasma frequency and γ is the Lorentz factor. The light frequency, ω_e , as seen by the electron is Doppler shifted, $\omega_e = \omega - kv$, where ω is the actual light frequency and v the electron velocity along the channel axis. Initially $\gamma = 2-3$ so that v is close to the light speed. An electron initially ahead of the pulse will be overtaken by the pulse due to its lower speed and thereby slightly accelerated. Eventually resonance occurs, $\omega_{\perp} \approx \omega_e$. Since this situation can be maintained for many light periods, the electron can pick up an appreciable amount of energy from the laser \mathbf{E} -field. The $\mathbf{v} \times \mathbf{B}$ action of the laser magnetic field converts this energy into longitudinal acceleration. The electron becomes then faster than the pulse, moves ahead of it, and finally drops out of resonance.

4. References

- [1] SAEMANN, A., et al., "Isochoric Heating of Solid Aluminum by Ultrashort Laser Pulse Focused on a Tamped Target", Phys. Rev. Lett. 82 (1999) 4843-4846.
- [2] WOOLSEY, N. C., et al., "Competing effects of collisional ionization and radiative cooling in inertially confined plasmas", Phys. Rev. E 57 (1998) 4650-4662.
- [3] MANCINI, R. C., et al., "Calculational aspects of the Stark line broadening of multi-electron ions in plasmas", Comp. Phys. Commun. 63 (1991) 314-322.
- [4] TABAC, M., et al., "Ignition and high gain with ultra-powerful lasers", Phys. Plasma 1 (1994) 1626-1634.
- [5] EIDMANN, K., et al., "Hydrodynamic simulation of subpicosecond laser interaction with solid-density matter", Phys. Rev. E 62, (2000) 1202-1214.
- [6] NGUYEN, H., et al., "Atomic structure and polarization line shift in dense hot plasmas", Phys. Rev. A 33 (1986) 1279-1290.
- [7] GAHN, C. et al., "Multi-MeV Electron Beam Generation by Direct Laser Acceleration in High-Density Plasma Channels", Phys. Rev. Lett. 83 (1999) 4772-4775.
- [8] TSAKIRIS, G., et al., "Laser induced electron acceleration in the presence of static electric and magnetic fields in a plasma", Phys. Plasma 7 (2000) 3017-3030.